

Analysis of harmonics currents in the case of grid connected photovoltaic generator

Habbati Bellia Assia^{1,3}, Moulay Fatima^{2,3}

¹Department of Electrical Engineering, Faculty of Technology, Tahri Mohamed University, Bechar, Algeria

²Department of Mechanical Engineering, Faculty of Technology, Djilali Liabès University, Sidi Bel Abbès, Algeria

³SGRE-Lab, Tahri Mohamed University, Bechar, Algeria

Article Info

Article history:

Received Feb 24, 2023

Revised Apr 20, 2023

Accepted May 3, 2023

Keywords:

Harmonics

Modulation index

Shit angle

Switching frequency

Synchronization

ABSTRACT

Nowadays, electrical grid experiences an increase in penetration of single-phase PV generations. Then, it becomes necessary to control this penetration by techniques of synchronization in order to provide electrical energy of good quality to the network. Estimation of the frequency, phase and magnitude of the grid voltage are necessary to correctly synchronizing the PV generator with grid. Connecting a direct current generator to grid via an inverter, requires to fix the performances to improve in the inverter to choose the best-suited topology. This paper describes the control of a non-isolated single-stage single-phase grid-connected inverter fed by a photovoltaic source. In order to define the influence of the three parameters: modulation index, switching frequency and phase shift angle, it is interesting to know the behavior of the system when one of these parameters moves away from its optimal value. Optimal values make it possible to obtain a THD as small as possible to satisfy the international standard. In this work, modulation index and switching frequency are set to their respective optimal values. To study grid current and inverter currents before and after filtering, harmonic analysis is performed for seven shift angles for the same switching frequency (10000 Hz) and modulation index (2.2).

This is an open access article under the [CC BY-SA](#) license.



Corresponding Author:

Habbati Bellia Assia

Department of Electrical Engineering, Faculty of Technology, Tahri Mohamed University

Bechar, Algeria

Email: bellia_abdeljalil@yahoo.fr

1. INTRODUCTION

The interest that science has brought to clean electricity of solar origin, has allowed a remarkable development in recent years of photovoltaic technology and each year, a considerable number of articles appear on the subject with all its ramifications. Journal articles help focus new research on actionable leads. However, this technology is still under development, and several new architectures appear each year. Barater *et al.* [1], which appeared in 2015, the authors worked on 53 articles (40 articles from the same database), the oldest of which appeared in 1981 and the most recent in 2014. In their comparative study, they presented a state of the art of converters dedicated to single-phase PV systems without transformer with measurement of the voltage between the terminals of the PV field and the ground. The waveform of this voltage allows adaptation between power converters and PV panels.

Another comparative study is presented in the article [2] published in 2020, also concerns the single-phase PV system without transformer. Authors carried out the study on 130 papers (1995-2019) and focused on the issue of safety. Common risks are earth fault currents, leakage currents and on compliance with the standards. They presented a detailed comparative study where they discussed in addition to the leakage

current; the cost, size, and efficiency. Authors represent an important classification in addition to a summarizing of a comparative study of the elements constituting the adaptation stage (inverter + filter) for 44 different topologies. The table provides another comparative study of the most used categories of transformer less single-phase inverters and offers an aid in identifying the respective advantages and limitations of different transformer less inverter topologies as it represents the main characteristics like common mode behavior, reactive power transfer capability, leakage current, efficiency and the number of components.

Alluhaybi *et al.* [3] worked on 90 articles (1999-2018) and classified the design of grid-connected photovoltaic micro inverters into four categories; according to the galvanic isolation (isolated or non-isolated) and according to the number of stages (one or two). In each of the four categories, the authors have chosen from the literature only the topologies that have been confirmed experimentally in terms of efficiency, power density, reliability, and cost. The criteria for comparison between topologies are implementation, battery integration, modular structure, number of components, and input voltage range. The study gave the superiority to single-stage micro inverters (with and without transformer) due to their simplicity and efficiency. However, single-stage transformer less topology offers low losses and lower cost compared to isolated topology. Besides, with a control scheme ensuring smooth switching operation for power switches, buck-boost remains the optimal solution for PV micro inverter design.

The article [4] is a state of the art of the photovoltaic conversion system. The author compared and analyzed the work of 56 papers (2002-2020). The two comparison criteria are also the galvanic isolation and the number of stages. In the case of a PV chain with transformer, the photovoltaic voltage can increase by placing a high frequency (HF) transformer on the DC side. However, to amplify the output voltage to the voltage values of the distribution network, a low frequency (LF) type transformer must be placed on the output side of the inverter. The major inconvenient of the inverter with transformer are losses, size and weight. While the major advantage is the galvanic isolation which ensures the safety of equipment and persons.

The PV inverter is a necessary element in the electro-energetic system connecting the photovoltaic source to the conventional electrical network. The conversion principle remains the same, but the topology of the chain changes depending on whether the integration takes place in the transmission network or in the distribution network. A photovoltaic power system is a chain made up of several elements and each plays a specific role. The chain must fulfill several sequential tasks, namely: conversion, adaptation and integration into the electrical network.

Increasingly, PV sources considered as dispersed production sources are being connected to the network and more particularly in its distribution part. Then, it requires interfacing them to the electrical network with inverters and in this paper, a single-stage single-phase inverter will connect the PV source to the network and a load. The point of common coupling (PCC) is the node that connects the load to the grid and to the output of the inverter. Then, the inverter must apply across of the load, a tension synchronized with the tension of the network. In this article, a single-phase single-stage inverter is chosen to interface the PV array to the grid. For this, it is necessary to control the power delivered by the inverter using a regulation loop that uses the network voltage as a reference.

Several simulations were made under MATLAB/Simulink to show the effect of the shift angle on the quality of current delivered by the inverter before and after filtering. The price of the filter increases with its size and if it is possible to reduce the harmonics before the filter, it will be possible to reduce the size of the inductances. The goal in this work is to separate the effect of the phase angle from that of the modulation index and the switching frequency in order to determine the harmonic levels targeted by a particular parameter.

2. DESCRIPTION OF THE PROPOSED SYSTEM

2.1. Power system description

The topology of the photovoltaic chain varies depending on whether the PV generator is connected to the medium or low voltage part of the electrical network. The use of the boost converter becomes essential if the DC source voltage is lower than the network voltage. On the other hand, the presence of the inverter is crucial since it allows converting direct current into alternative current. Since the aim of this study is analysis of currents at the PPC, it is preferable to adjust DC source voltage to an enough value to be equal to the voltage delivered by the grid and in this case, the converter DC/DC should not be used. The output of the DC source must be connected to the input of the inverter by using a DC link. The role of the inverter is to generate alternative voltage from sources providing direct voltages such as fuel cell, batteries or photovoltaic generators. This power can be injected into the electrical grid or supply a load because it can be connected to the load at the same time as the grid. For this, it is essential to synchronize the voltage delivered by the inverter with the grid voltage. Figure 1 shows the standard one stage topology of the power system. PCC relays the load to the grid and the inverter output.

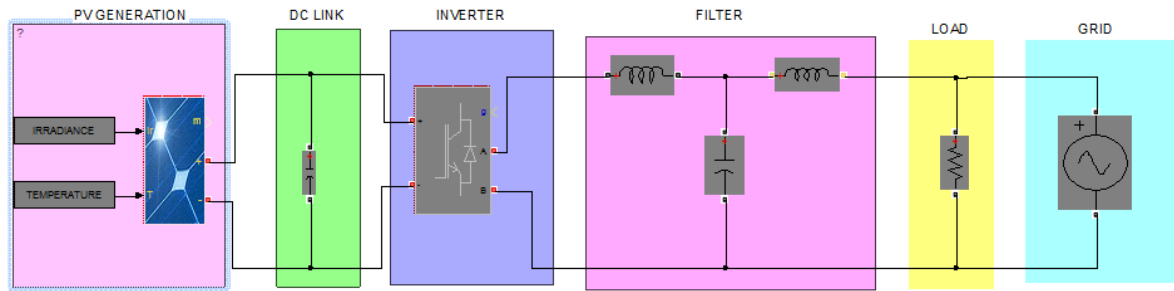


Figure 1. Standard topology of single-stage single-phase grid connected PV system

2.2. Control description

The control system is presented in Figure 2 as a synoptic diagram. To synchronize PV array with electrical grid, the voltage grid is used as an input to the PLL bloc. The PLL bloc output is used with index modulation m_a and shift angle to build the reference sine wave. U_{ref} is compared with carrier wave in PWM bloc to generate pulses.

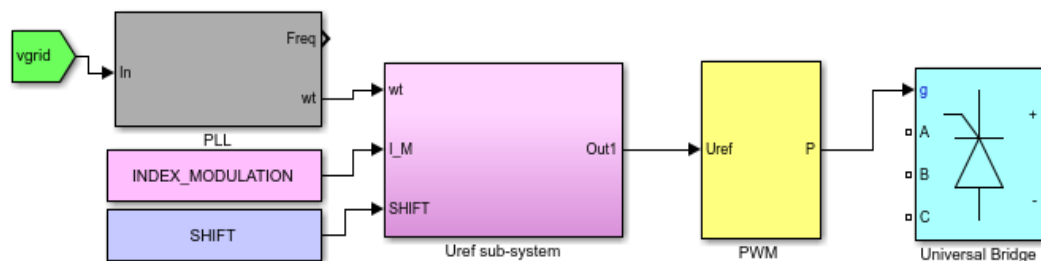


Figure 2. Synoptic diagram of the control system

2.2.1. Inverter

In this paper, Inverter is a Universal bridge (IGBT) controlled by PWM. Therefore, it is interesting to remember that IGBT technology is chosen for [5], [6]: i) Very high switching power which enables the output signal to be as close as possible to the sinusoidal shape; ii) High current which enables it to supply loads such as motors modeled in series RL circuit; and iii) Control in voltage and not in current to avoid switching losses.

2.2.2. Pulse width modulation PWM

The grid fundamental frequency (either 50 Hz or 60 Hz) is used as an input variable to obtain the reference sinusoidal wave. the reference wave is then compared with a carrier triangular wave at the switching frequency to produce pulses at the intersection points. The switching frequency has a considerable effect on the switching cells of the inverter since it affects the harmonic content [7]–[9]. Therefore, the switching frequency must be well chosen to reduce the harmonics. IEC and IEEE standards suggest that PV system output should have low current-distortion levels to ensure security of other equipment connected to the utility system as described in [10], [11]. Total harmonic current distortion shall be less than 5% at rated inverter output. Both references present table of limits for individual harmonic. Also, even harmonics shall be less than 25% of the lower odd harmonic limits listed.

2.2.3. Phase locked loop PLL

In general, PLL is used as a part of control system and whose output signal is synchronized in phase, in frequency with the fundamental voltage component of the grid. PLL provides synchronization information with protection against harmonics and other disturbances. The word [12] summarizes in a table different single-phase PLL based techniques already published in literatures. Table 1 classifies the synchronization techniques into two types: PLL based methods non-PLL based methods.

Table 1. Classification of single-phase grid synchronization techniques [12]

PLL based methods	Non-PLL based methods
T/4 delay	Fourier analysis
Inverse park's transform	inducverter
Enhanced	
Robust PLL	
SOGI	

2.2.4. Index modulation

Many indexes are cited in literature but the most important in this case is the modulation index (ma) which is defined as the ratio of amplitudes of the reference wave to the triangular wave [13]–[16].

$$ma = \frac{U_{ref}}{U_t} \quad (1)$$

U_{ref} reference wave amplitude, U_c triangular wave amplitude.

2.2.5. Power decoupling

These power-decoupling techniques are categorized into three groups in terms of the decoupling capacitor locations: 1) PV-side decoupling; 2) DC-link decoupling; and 3) AC-side decoupling. Power decoupling is achieved by means of an electrolytic capacitor but can be substituted with film capacitors because of the lifetime problem. In this work, the capacitor is placed in parallel with the PV modules in the dc link, between the PV array and inverter stage as can be seen in Figure 1. According to [17], [18], the size of the decoupling capacitor is expressed as (2).

$$C = \frac{P_{PV}}{2 \cdot \omega_{grid} \cdot V_{DC} \cdot \hat{u}_c} \quad (2)$$

P_{PV} is the nominal power of the PV modules, V_{DC} is the mean voltage across the capacitor, \hat{u}_c is the amplitude of the ripple.

3. MODELLING AND SIMULATION

To synchronize PV array with electrical grid, the grid voltage is used as an input to the PLL bloc. The output PLL bloc is used with index modulation ma and shift angle to build the reference sine wave. U_{ref} is compared with carrier wave in PWM bloc to generate pulses. The modeling of the LCL filter must take into consideration variables which concern on the one hand the inverter such as the nominal power and the switching frequency and on the other hand the network such as its nominal voltage and its frequency. The base impedance, Z_B , and base capacitance, C_B , are then defined as [19]–[21]:

$$Z_B = \frac{V_n^2}{S_n} \quad (3)$$

$$C_B = \frac{1}{\omega_n Z_B} = \frac{1}{2 \cdot \pi \cdot f \cdot Z_B} \quad (4)$$

Since the filter capacitor value is based on the reactive power absorbed at the rated condition and is referred to in a percentage of the base capacitor value $C_{fmax} = 5\%$ of C_B .

$$C_{fmax} = \frac{0.05}{2 \cdot \pi \cdot f \cdot \frac{V_n^2}{S_n}} = \frac{0.05 \cdot S_n}{2 \cdot \pi \cdot f \cdot V_n^2} \quad (5)$$

The filter can contain one or two inductors depending on the chosen topology: L, LC or LCL. In this paper, the LCL filter has been chosen. The inductor connected to the inverter is defined as the inverter side inductor. It concerns on maximum permissible current ripple that is limited to 20% of the rated current. The inductor size can be expressed as:

$$L_{inv} = \frac{V_{DC}}{4 \cdot \Delta I_{max} \cdot f_s} \quad (6)$$

where V_{DC} represent the dc link voltage [22]–[24].

$$r = \frac{L_{grid}}{L_{inv}} \quad (7)$$

The total inductance is selected according to the maximum voltage drop across the inductor. As the upper limit on the fundamental voltage drop as 10%, [25] the total inductor is expressed:

$$L_{inv} + L_{grid} \leq 10\%L_b \quad (8)$$

$$V_{L_1+L_2} = I \cdot 2 \cdot \pi \cdot f \cdot (L_{inv} + L_{grid}) = 0.1 V \quad (9)$$

$$L_{inv} + L_{grid} = \frac{0.1V^2}{S \cdot 2 \cdot \pi \cdot f} \quad (10)$$

The inductor connected to the grid can be calculated by subtraction from the equation. The resonance frequency of the LCL-filter can be expressed as (11) [26], [27].

$$f_{res} = \frac{1}{2 \cdot \pi} \sqrt{\frac{(L_{grid} + L_{inv})}{L_{grid} L_{inv} C_{fmax}}} \quad (11)$$

Moreover, the resonance frequency must satisfy the inequality:

$$10f_{grid} < f_{res} < 0.5f_s \quad (12)$$

the Table 2 summarizes system specification used in simulation

Table 2. System specification used in simulation

Parameters	Value
Grid voltage	230 V
Grid frequency	50 Hz
Open circuit voltage of PV array	400 V
DC bus voltage	375 V
Rated power	2000 W
Current ripple	20%

4. RESULTS AND ANALYSIS

Simulation has been done under MATLAB/Simulink environment. After running simulation, the output voltage of the inverter represented in Figure 3, is three level $(-V_{in} \ 0 \ +V_{inv})$ periodic but not sinusoidal. The peak value is equal to the direct voltage of 380 V. The Figure 4 shows the synchronization between grid voltage V_{grid} and inverter voltage V_{inv} after setting the following parameters as follows: $f_s=10000$ Hz $ma=0.85$ shift=2, it should be noted that in this simulation, the time required for synchronization is 0.04 s. The Figure 5 represents the synchronization between the different voltages (grid, inverter, and load) and their respective currents.

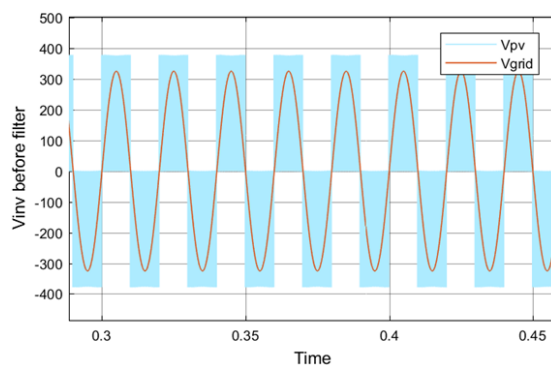


Figure 3. voltage waveform at the output of inverter compared with grid voltage waveform

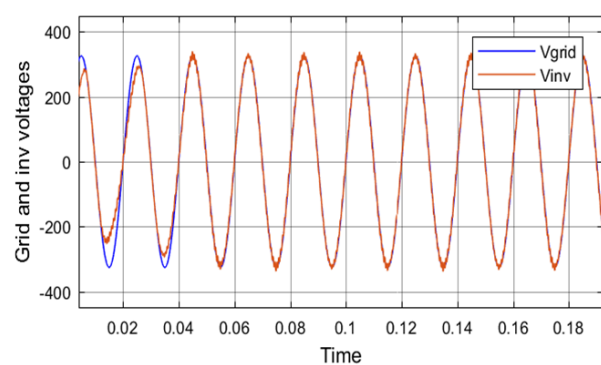


Figure 4. Wave form of the grid voltage and inverter voltage after filtering

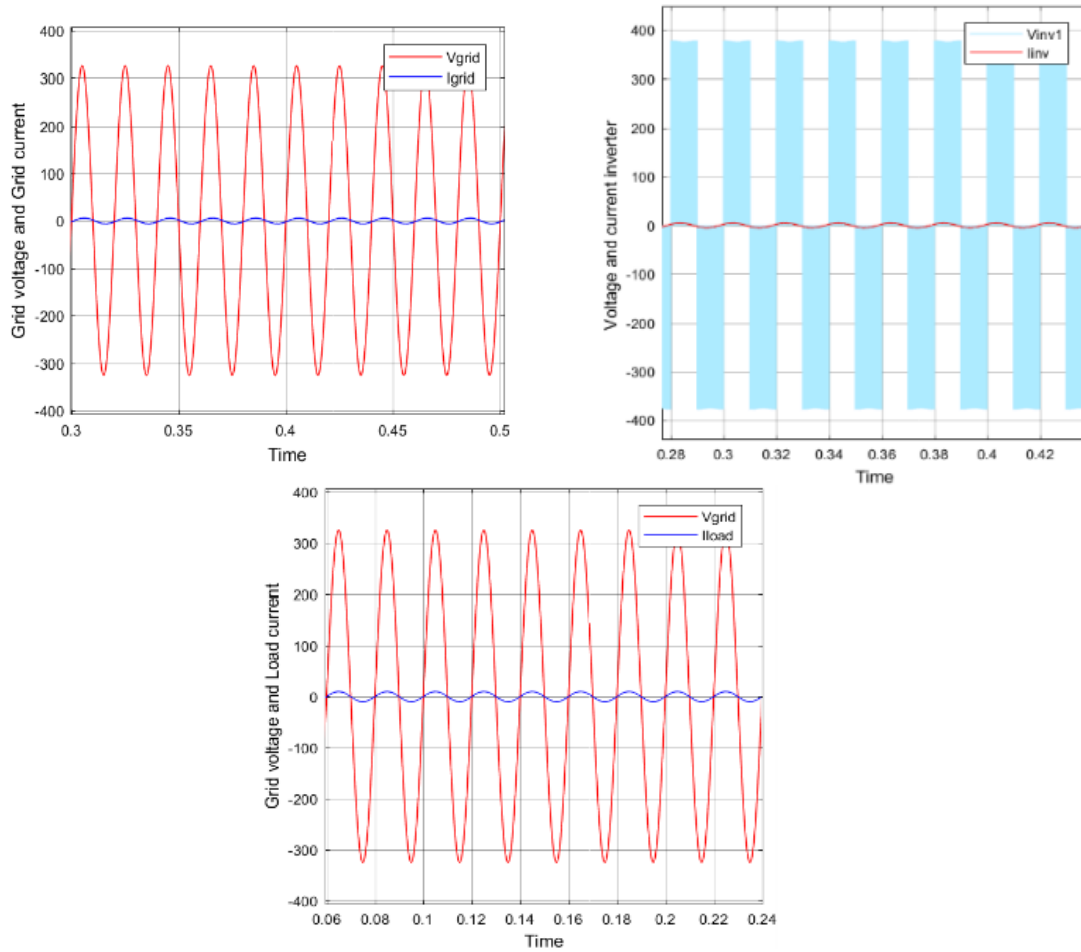


Figure 5. Phase shift between voltages and currents in: grid, inverter, and load

The Figure 6 represents plots of all currents circulating in the power system. For each current, we represent the waveform and the FFT waveforms of currents in Figure 6(a) is grid, Figure 6(b) is inverter before filter, Figure 6(c) is load, and Figure 6(d) is after filter. Simulation has been done for the values already mentioned. THD values meet the requirement of currents and recommendations. THD of output inverter voltage is relatively high and above the limit but is attenuated by the filter.

In Figure 7, we can see the synchronization between the grid voltage waveform and the reference waveform. The PLL uses the grid voltage as the input voltage to slave the frequency of the voltage. This frequency will be used to obtain a reference voltage whose amplitude varies between -1 and +1. This frequency voltage should be injected into the PWM to obtain the inverter control signal.

The phase shift controls the active power and then the current needed to supply the load completed by the current provided by the grid. The current of the load was fixed previously at 10 amperes by fixing active power. In test simulations not presented in paper, the current was provided by grid when disconnecting the DC source and by the DC by disconnecting the grid. It is the sum of both currents when the grid and the DC current are connected together with the load according to Kirchhoff's current law.

In order to show the influence of the phase shift on the composition of the current wave, a tracing of the THD was carried out by modifying the parameter α around the optimal value. The Figure 8 shows the shape of the curves as a function of the change in phase shift. By changing α , the phase shift is changing too. α is the parameter that intervenes in the calculation of the phase shift angle.

$$U_{ref} = ma \cdot \sin(\omega t + \varphi) = ma \cdot \sin(\omega t + \alpha \cdot \pi / 180) \quad (13)$$

The curves in the Figure 9 show the variation of THD as a function of the phase shift for the grid current, the inverter current before and after the filtering. The optimal values of the modulation index and of the switching frequency are necessary to highlight the intervention of the phase shift. Switching frequency has been fixed to 10000 Hz and modulation index to 0.85.

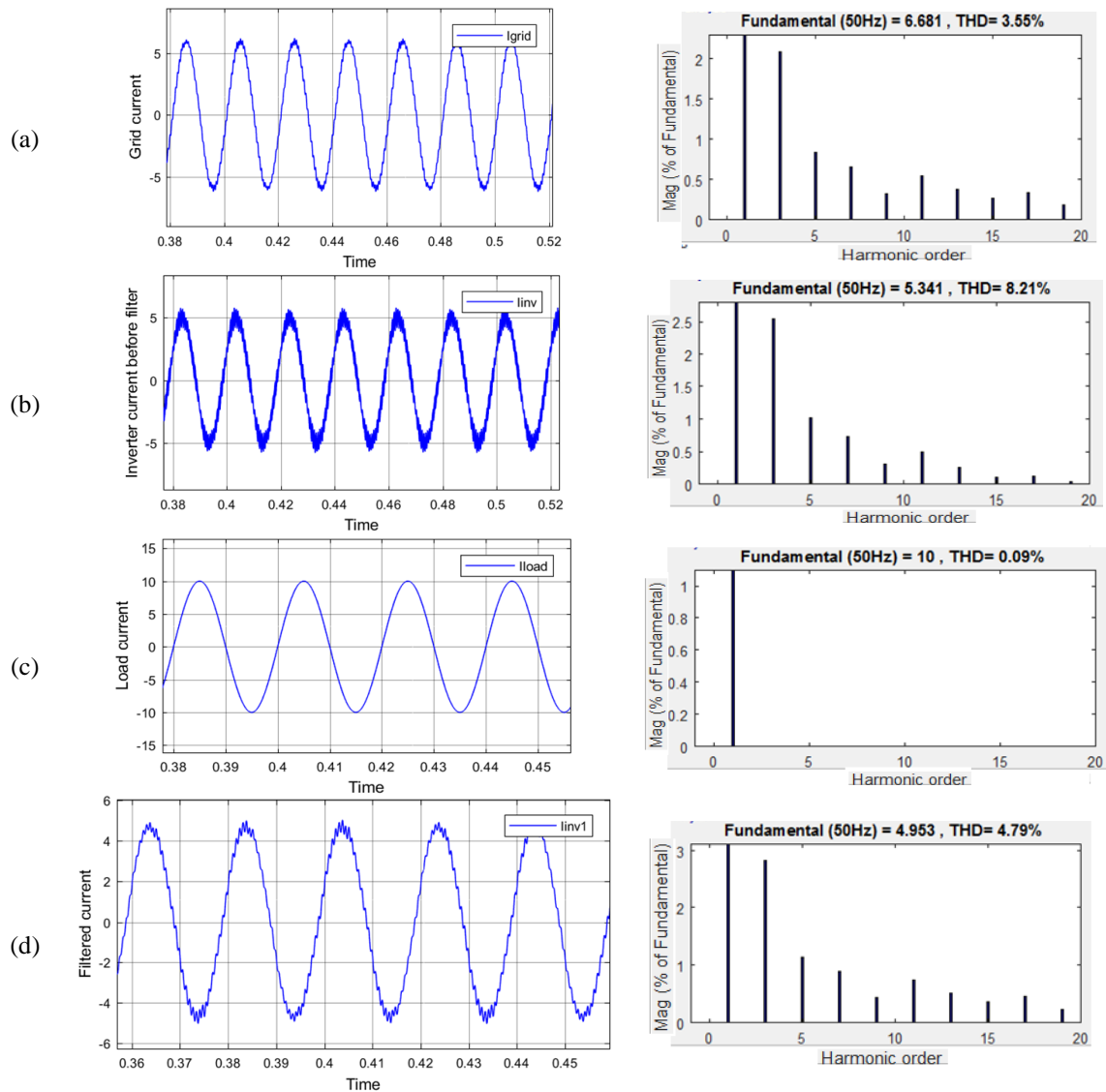


Figure 6. Harmonic analysis for currents at $f_s=10000$ Hz, $ma=0.85$, $shift=2.2$: (a) FFT and plot of grid current, (b) FFT and plot of inverter current, (c) FFT and plot of load current, and (d) FFT and plot of filtered current

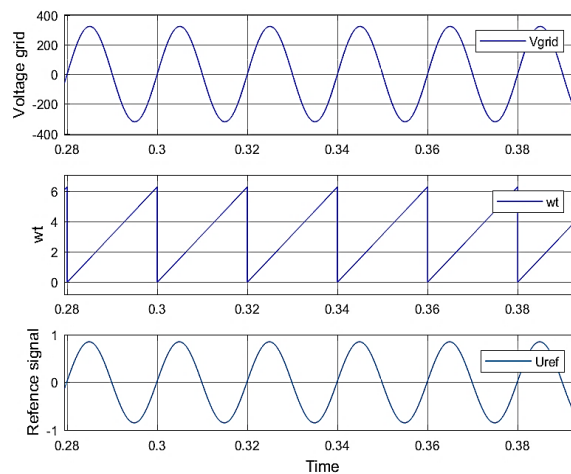
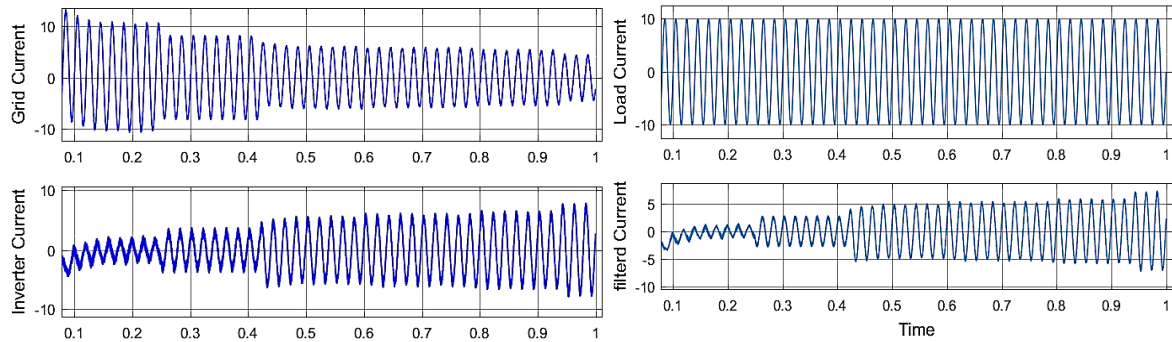
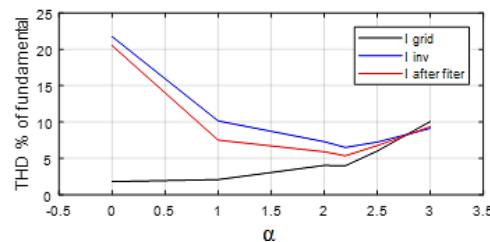


Figure 7. Reference and ωt waveforms

Figure 8. Shape of the current curve α : 0, 1, 2, 2.2, 2.5, 3Figure 9. THD vs α for currents at PCC

For $\alpha < 2.2$, even after filter, the THD of the inverter current remains above the recommended limits ($>5\%$). While the current THD in the grid is low. It is the value $\alpha = 2.2$ which makes it possible to attenuate the harmonics before and after the filtering at the lowest of their values. This value allows two major conclusions to be drawn: i) The filter is not solely responsible for the drop-in harmonics; and ii) It is possible to reduce the size of the filter and its price by reducing the harmonics to their minimum possible by regulating the cut-off frequency and the modulation index before filtering. Thus, the filter intervenes to reduce the persistent harmonics until the standards and recommendations are met.

5. CONCLUSION

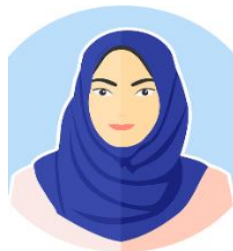
The paper has analyzed the behavior of the currents at PCC in a single-phase single stage grid connected PV system when varying the three important parameters: index modulation, phase shift and swift frequency. A control loop containing PLL, U_{ref} sub-system and PWM, synchronized successfully the inverter with the grid. The simulation in MATLAB/Simulink environment has allowed a detailed analysis of THD variation when varying one of the three parameters. The proposed control loop shows that by keeping constant the modulation index and the switching frequency, the variation of α gives one point ($\alpha = 2.2$) where THD is less than 5% for inverter current after filtering (4.79%) and for grid current simultaneously. This point represents the optimal value of phase shift.




REFERENCES

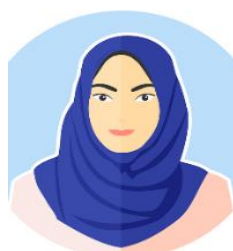
- [1] D. Barater, E. Lorenzani, C. Concar, G. Franceschini, and G. Buticchi, "Recent advances in single-phase transformerless photovoltaic inverters," *IET Renewable Power Generation*, vol. 10, no. 2, pp. 260–273, Feb. 2016, doi: 10.1049/iet-rpg.2015.0101.
- [2] M. N. H. Khan, M. Forouzesh, Y. P. Siwakoti, L. Li, T. Kerekes, and F. Blaabjerg, "Transformerless inverter topologies for single-phase photovoltaic systems: a comparative review," *IEEE Journal of Emerging and Selected Topics in Power Electronics*, vol. 8, no. 1, pp. 805–835, Mar. 2020, doi: 10.1109/JESTPE.2019.2908672.
- [3] K. Alluhaybi, I. Batarseh, and H. Hu, "Comprehensive review and comparison of single-phase grid-tied photovoltaic microinverters," *IEEE Journal of Emerging and Selected Topics in Power Electronics*, vol. 8, no. 2, pp. 1310–1329, Jun. 2020, doi: 10.1109/JESTPE.2019.2900413.
- [4] M. Bouzguenda and T. Selmi, "Review of DC-AC converters for photovoltaic conversion chains," *International Journal of Power Electronics and Drive Systems (IJPEDS)*, vol. 12, no. 2, p. 886, Jun. 2021, doi: 10.11591/ijpeds.v12.i2.pp886-901.
- [5] E. M. Findlay and F. Udrea, "Reverse-conducting insulated gate bipolar transistor: a review of current technologies," *IEEE Transactions on Electron Devices*, vol. 66, no. 1, pp. 219–231, Jan. 2019, doi: 10.1109/TED.2018.2882687.
- [6] W. C. W. Hsu, F. Udrea, H. Y. Hsu, and W. C. Lin, "Reverse-conducting insulated gate bipolar transistor with an anti-parallel thyristor," in *Proceedings of the International Symposium on Power Semiconductor Devices and ICs*, 2010, pp. 149–152.
- [7] I. Isdawimah, R. Setiabudy, and R. Gunawan, "The effect of high switching frequency on inverter against measurements of kWh-




- meter,” *IPTEK Journal of Proceedings Series*, no. 1, Dec. 2014, doi: 10.12962/j23546026.y2014i1.531.
- [8] X. Wen and X. Yin, “The unified PWM implementation method for three-phase inverters,” in *2007 IEEE International Electric Machines & Drives Conference*, May 2007, pp. 241–246, doi: 10.1109/IEMDC.2007.383584.
- [9] J.-D. Zhang, F. Peng, Y.-K. Huang, Y. Yao, and Z.-C. Zhu, “A novel low control frequency control strategy of high switching frequency inverter for high speed PMSM current control,” in *2020 International Conference on Electrical Machines (ICEM)*, Aug. 2020, pp. 2358–2364, doi: 10.1109/ICEM49940.2020.9270806.
- [10] G. S. Rani and R. Ahemmed, “Switching frequency harmonic selection for single phase multilevel cascaded h-bridge inverters,” *International Journal of Electrical and Electronics Engineering Research (IJEER)*, vol. 3, no. 2, pp. 24–260, 2013.
- [11] IEC 61727, *Photovoltaic (PV) systems – characteristics of the utility interface*. 2004.
- [12] I. 1547, *Standard for interconnecting distributed resources with electric power systems*. 2003.
- [13] R. R. Behera and A. N. Thakur, “An overview of various grid synchronization techniques for single-phase grid integration of renewable distributed power generation systems,” in *2016 International Conference on Electrical, Electronics, and Optimization Techniques (ICEEOT)*, Mar. 2016, pp. 2876–2880, doi: 10.1109/ICEEOT.2016.7755223.
- [14] M. E. Asker and Heybet Kiliç, “Modulation index and switching frequency effect on symmetric regular sampled SPWM,” *European Journal of Technic*, vol. 7, no. 2, pp. 102–109, Dec. 2017, doi: 10.23884/ejt.2017.7.2.04.
- [15] A. Al-Hasani, M. Abouelela, S. Alghuwainem, A. M. Al-Shaalan, and Y. Bakhuraisa, “The effect of modulation index in THD of transformer less inverter,” *Test Engineering and Management*, vol. 82, no. February 2021, pp. 5691–5697, 2020.
- [16] K. Kanagavel and C. Govindaraju, “Adaptive single carrier multilevel modulation for grid connected single phase modular multilevel inverter,” *Journal of Ambient Intelligence and Humanized Computing*, Apr. 2021, doi: 10.1007/s12652-021-03087-y.
- [17] S. B. Kjaer, J. K. Pedersen, and F. Blaabjerg, “A review of single-phase grid-connected inverters for photovoltaic modules,” *IEEE Transactions on Industry Applications*, vol. 41, no. 5, pp. 1292–1306, Sep. 2005, doi: 10.1109/TIA.2005.853371.
- [18] M. Repak, A. Otcenasova, J. Altus, and M. Regula, “Grid-tie power converter for model of photovoltaic power plant,” *Electrical Engineering*, vol. 99, no. 4, pp. 1377–1391, Dec. 2017, doi: 10.1007/s00202-017-0611-6.
- [19] N. A. Sabran, C. L. Toh, and C. W. Tan, “LCL-filter design and analysis for PWM recuperating system used in DC traction power substation,” *International Journal of Power Electronics and Drive Systems (IJPEDS)*, vol. 13, no. 4, p. 2244, Dec. 2022, doi: 10.11591/ijpeds.v13.i4.pp2244-2254.
- [20] A. Reznik, M. G. Simoes, A. Al-Durra, and S. M. Mueen, “LCL filter design and performance analysis for grid-interconnected systems,” *IEEE Transactions on Industry Applications*, vol. 50, no. 2, pp. 1225–1232, Mar. 2014, doi: 10.1109/TIA.2013.2274612.
- [21] M. Liserre, F. Blaabjerg, and S. Hansen, “Design and control of an LCL-filter-based three-phase active rectifier,” *IEEE Transactions on Industry Applications*, vol. 41, no. 5, pp. 1281–1291, Sep. 2005, doi: 10.1109/TIA.2005.853373.
- [22] J. Sedo and S. Kascak, “Design of output LCL filter and control of single-phase inverter for grid-connected system,” *Electrical Engineering*, vol. 99, no. 4, pp. 1217–1232, Dec. 2017, doi: 10.1007/s00202-017-0617-0.
- [23] C. Poongothai and K. Vasudevan, “Design of LCL filter for grid-interfaced PV system based on cost minimization,” *IEEE Transactions on Industry Applications*, vol. 55, no. 1, pp. 584–592, Jan. 2019, doi: 10.1109/TIA.2018.2865723.
- [24] M. F. Yaakub, M. A. M. Radzi, M. Azri, and F. H. M. Noh, “LCL filter design for grid-connected single-phase flyback microinverter: a step by step guide,” *International Journal of Power Electronics and Drive Systems (IJPEDS)*, vol. 12, no. 3, p. 1632, Sep. 2021, doi: 10.11591/ijpeds.v12.i3.pp1632-1643.
- [25] J. Selvaraj, N. A. Rahim, and C. Krismadinata, “Digital PI current control for grid connected PV inverter,” in *2008 3rd IEEE Conference on Industrial Electronics and Applications*, Jun. 2008, pp. 742–746, doi: 10.1109/ICIEA.2008.4582614.
- [26] N. Ismail, A. Permadi, A. Risdiyanto, B. Susanto, and M. A. Ramdhani, “The effect of amplitude modulation index and frequency modulation index on total harmonic distortion in 1-phase inverter,” *IOP Conference Series: Materials Science and Engineering*, vol. 288, p. 012107, Jan. 2018, doi: 10.1088/1757-899X/288/1/012107.
- [27] H. Hu, S. Harb, N. Kutkut, I. Batarseh, and Z. J. Shen, “A review of power decoupling techniques for microinverters with three different decoupling capacitor locations in PV systems,” *IEEE Transactions on Power Electronics*, vol. 28, no. 6, pp. 2711–2726, Jun. 2013, doi: 10.1109/TPEL.2012.2221482.

BIOGRAPHIES OF AUTHORS



Habbati Bellia Assia    is lecturer in Electrical Engineering Department, Tahri mohamed University Béchar, Algeria since 2008; and she has been a senior lecturer since 2015. She received the Engineer degree in electrical engineering and the Magister degree in electrotechnics, both from Djilali Liabes University, Sidi Bel Abe, Algeria, in 1990 and 2007, respectively; and Ph.D. degree in Electrical Power Engineering from the same university in 2014. Her research interests include the field of electrical power, industrial applications, photovoltaic power systems, digital design. She can be contacted at email: bellia_abdeljalil@yahoo.fr.



Moulay Fatima    is lecturer in Mechanical Engineering Department, Djilali Liabes University, Sidi Bel Abe, Algeria since 2002; and she has been a senior lecturer since 2014. She received the Engineer degree in electrical engineering and the Magister degree in electrotechnics, both from Djilali Liabes University, Sidi Bel Abe, Algeria, in 1990 and 2002, respectively; and Ph.D. degree in Electrical Power Engineering from the same university in 2014. Her research interests include the field of electrical power, motor drives, industrial applications, digital design. She can be contacted at email: fatimamoulay66@yahoo.fr.